AIMS Energy, 14(1): 140–160.
DOI: 10.3934/energy.2026006
Received: 22 August 2025
Revised: 15 December 2025
Accepted: 17 December 2025
Published: 19 January 2026

https://www.aimspress.com/journal/energy

Research article

Dynamic adjustment strategy for an integrated 'wind-solar-storage' power station based on digital twin

Xiancheng Cui[1], Xiaoming Lu[1], Yiwen Yao[1], Xin Xu[1], Meihan Liu[2] and Jingjie Zhao[2,*]

[1] Jilin Province Changchun Electric Power Survey and Design Institute Co., Ltd, Changchun, China
[2] School of Business and Management, Jilin University, Changchun, China

* **Correspondence:** Email: zjj@jlu.edu.cn.

Abstract: As the share of new energy generation increases, its intermittent and uncertain nature threatens the stability of power systems. This study introduces a dynamic scheduling approach for wind-solar storage-charging hybrid power stations utilizing digital twin technology. By constructing an accurate virtual model of physical entities, the approach enables real-time monitoring, simulation analysis, and intelligent optimal control of the power system, providing a new solution for improving power station operation efficiency and power grid stability. In this application scenario, the digital twin system integrates and analyzes the operation data of the power station and optimizes the node voltage control and peak shaving control strategies of the energy storage power station. Regarding node voltage regulation, the reactive power output is dynamically fine-tuned in line with energy storage's charge-discharge attributes, with the ideal charge-discharge power identified via the particle swarm optimization (PSO) algorithm and digital twin simulation capability. Simulation results show that the node voltage fluctuation of the traditional strategy is ± 5% with 8 over-limits, while the proposed strategy reduces it to ± 2% with 1 over-limit. In peak shaving control, through digital twin simulation and PSO for energy storage capacity configuration, the optimal charging and discharging plan is determined, reducing the grid peak-valley difference from 30% of the traditional strategy to 15%. In conclusion, this strategy has significant advantages in improving the efficiency of new energy power stations and power grid stability, providing technical support for building a clean and efficient energy system.

Keywords: wind-solar energy storage; node voltage control; peak shaving strategy; digital twin; PSO algorithm

1. Introduction

The proportion of new energy generation in the global energy structure continues to rise. The International Energy Agency (IEA) predicts that new energy's share will increase from approximately 20% to 40% by 2030 [1]. Nevertheless, new energy's intermittent and uncertain characteristics present challenges for the stable functioning of power systems. Conventional scheduling and operational models fail to accommodate the intricate shifts following extensive new energy integration, leading to increased difficulties in grid frequency and voltage control, and may even trigger stability crises [2,3].

To tackle this problem, digital twin technology has progressively emerged as a focal research area in power systems. Numerous researchers have delved into applying digital twin technology in power grid systems. Ismail et al. [4] pointed out that digital twin solutions are essential to address challenges in the energy supply sector and comprehensively analyzed the technology's applications therein. Liu et al. [5] proposed a digital twin modeling method for data integration and efficient management during the operation and maintenance phase of NZEB. Zhao et al. [6] proposed an innovative strategy for urban microgrid (MG) management and socioeconomic development, focusing on improving energy efficiency and reliability and promoting net-zero emission goals. Singh et al. [7] proposed an intelligent anomaly detection technique for a software-defined IoT (SDN-IoT) environment supporting digital twins. By leveraging the capabilities of software-defined networking, the network can be reconfigured according to rules specified by the controller.

Parada et al. [8] proposed a hierarchical digital control strategy for managing distribution power systems, using battery energy storage systems (BESS) to regulate voltage amplitude and improve overall performance, achieving efficient energy management. Inaolaji et al. [9] developed an optimization model to determine and optimize the capacity and location of BESS connected to the distribution network, aiming to achieve two key service options: peak shaving and reliability enhancement, while considering both normal operation and outage scenarios. Liang et al. [10] proposed a novel fault identification method based on wavelet packet energy spectrum and a convolutional neural network (CNN), effectively addressing the problem of feature extraction for complex faults in hybrid DC transmission systems. Ouyang et al. [11] studied the application of vanadium redox flow battery-based microgrids in rural areas, integrating biomass gasification and solid oxide fuel cells as power generation units to provide stable electricity.

While the aforementioned methods have eased new energy integration issues, they possess certain constraints: conventional node voltage control lacks sufficient precision and responsiveness, struggling to satisfy voltage stability demands post large-scale new-energy integration. Current peak shaving strategies do not adequately account for new energy's uncertainty, resulting in limited peak shaving effects and still large peak-valley differences [12]. To this end, this paper proposes a digital-twin-enabled dynamic scheduling strategy for integrated "wind–PV storage-charging" power plants. First, a closed-loop digital-twin framework is established to realize bidirectional real-time mapping between the physical and virtual domains of the plant. Second, the particle swarm algorithm is embedded into the twin, coordinately optimizing both reactive and active storage outputs for voltage regulation and peak-load shaving. Third, online twin-based simulations replace traditional offline models, enabling rolling

closed-loop corrections of nodal voltages and peak-shaving strategies. By constructing a high-fidelity virtual replica, the approach achieves full-coverage monitoring, simulation-based analysis, and intelligent optimal control, thereby enhancing renewable plant efficiency and grid stability and offering a novel solution to pertinent challenges.

2. Construction of the digital twin system for wind-solar storage-integrated power stations

Against the backdrop of energy transition and sustainable development, wind-solar hybrid power plants occupy a crucial position in the new energy sector, and their stable and efficient operation is of paramount importance [13]. The digital twin model for wind-solar hybrid power plants constructed in this paper, which is based on advanced information technology and energy management concepts, boasts unique construction principles, powerful functions, and significant advantages. It introduces novel methods for the optimal management of power plants, significantly drives the advancement of the new energy industry, and holds substantial importance in enhancing the operational performance of wind-solar hybrid power plants. The structure of the digital twin technology is illustrated in Figure 1. Each sensor listed in the perception layer—wind turbine, PV, and storage nodes—maps one-to-one to the actual injection points in the IEEE 33-bus system of Figure 2. The data-stream bandwidth and sampling period between the edge and twin layers directly determine whether the PSO algorithm of Section 3.1 can finish the rolling update of 42 PMU channels and 128 thermal-control signals within 1 min. Finally, the closed-loop arrows between the application and physical layers correspond to the real-time dispatch paths for reactive-power Qref (Section 3.2) and charge/discharge power Pref (Section 3.3), guaranteeing that the simulation outcomes—voltage swing reduced from ± 5% to ± 2% and peak-to-valley difference from 30% to 15%—are physically attainable.

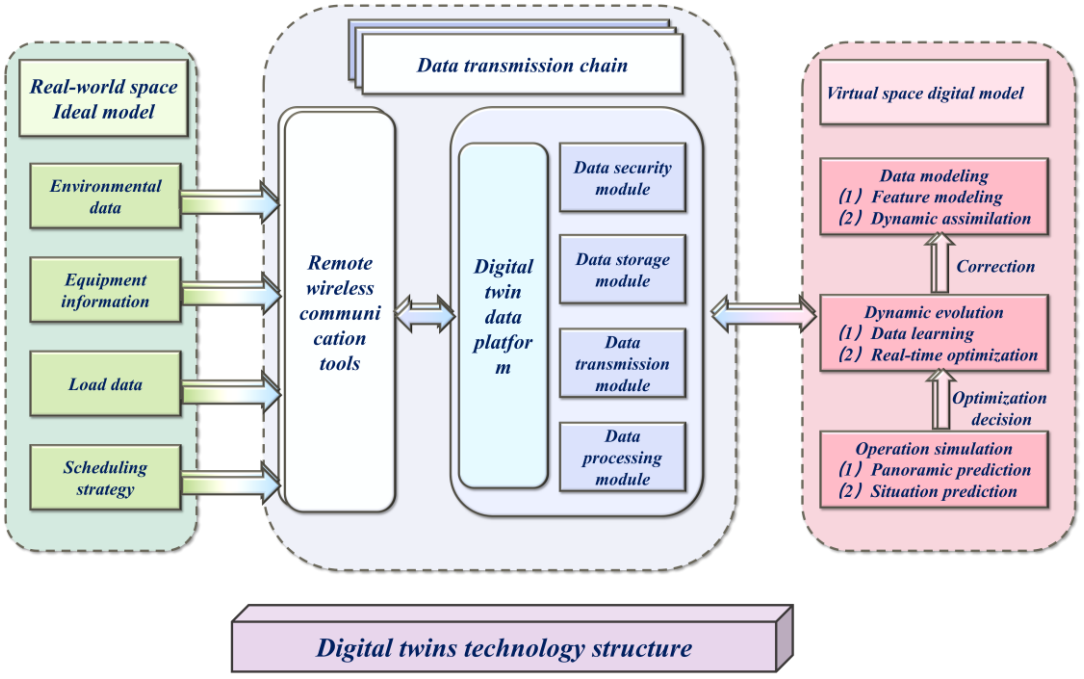

Figure 1. Structure of the digital twin technology.

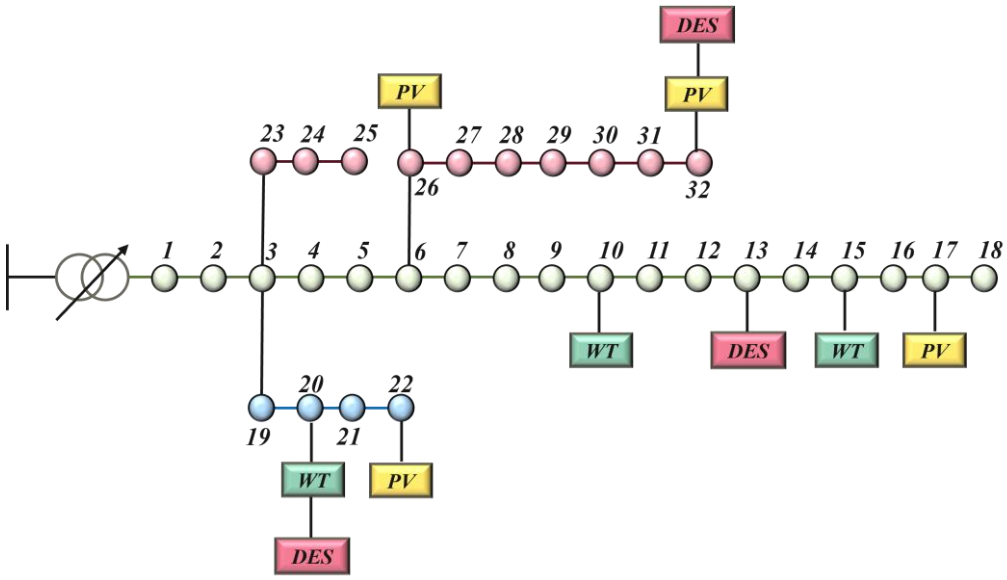

Figure 2. System line diagram of the improved IEEE 33-node system.

This construction of the digital twin model for wind-solar hybrid power stations adheres to the fundamental principle of virtual-real mapping and integration [14], with its model architecture shown in Figure 3. At the physical entity level, various devices of the wind-solar hybrid power station form the physical entity foundation. These sensors collect in real-time multi-source heterogeneous data, including wind speed, wind direction, illumination intensity, and equipment operating parameters, and transmit the data to the digital space through a stable and reliable communication network. In the digital space, a virtual model corresponding to the physical entity is constructed using high-precision 3D modeling technology. This model not only highly resembles the physical entity in appearance but also achieves accurate mapping in terms of internal structure, performance parameters, and other aspects. Meanwhile, advanced data processing algorithms and physics engines are employed to analyze, fuse, and simulate calculations on the real-time transmitted physical entity data, allowing the virtual model to dynamically mirror the operational conditions of the physical entity across various working scenarios. As a result, this enables real-time interaction and synchronous updates between physical entities and digital models, thereby establishing a robust groundwork for the subsequent realization of functions under various operating conditions [15]. This study further introduces a multi-domain unified modeling method based on Modelica-FMI, which encapsulates the coupled dynamic characteristics of wind, solar, energy storage, and power grid into FMU (functional mock-up unit) modules, enabling variable-step simulation on a millisecond-to-minute scale. An MQTT + Kafka asynchronous bus is deployed to achieve bidirectional data synchronization between the lightweight digital twin based on Docker at the edge side and the high-fidelity model based on Kubernetes in the cloud, with end-to-end latency controlled below 50 ms. To ensure the feasibility and reliability of this latency indicator, this study adopts Intel Xeon D-2750 edge computing nodes suitable for industrial edge scenarios (low power consumption, high real-time performance) and industrial-grade 5G communication modules compliant with 3GPP Release 16 (based on the OPC UA protocol, with downlink rate $\geq$ 500 Mbps and uplink rate $\geq$ 100 Mbps); a high-precision timestamp capture method based on NTP synchronization (synchronization error $\leq$ 1 ms) is used to calculate the total end-to-end latency from physical data collection to simulation result feedback. A dual-clock mechanism is designed—including a

Kalman-corrected real-time clock (1 s) and an LSTM parameter-updated evolution clock (1 h)—to control the virtual-physical state deviation within 0.5%. According to GB/T 39958-2021 General Requirements for Digital Twins in Industrial Processes, this deviation is calculated through the relative error between measured values and simulated values of core operating parameters (wind turbine speed, photovoltaic output, and energy storage SOC). OPC UA-TLS 1.3 encryption and DTID-based digital thread tracing technology are adopted to ensure end-to-end consistency across the entire sensor-model-controller link, achieving an MTBF (mean time between failures) of > 8000 h, which meets the strict reliability requirements of power station operation.

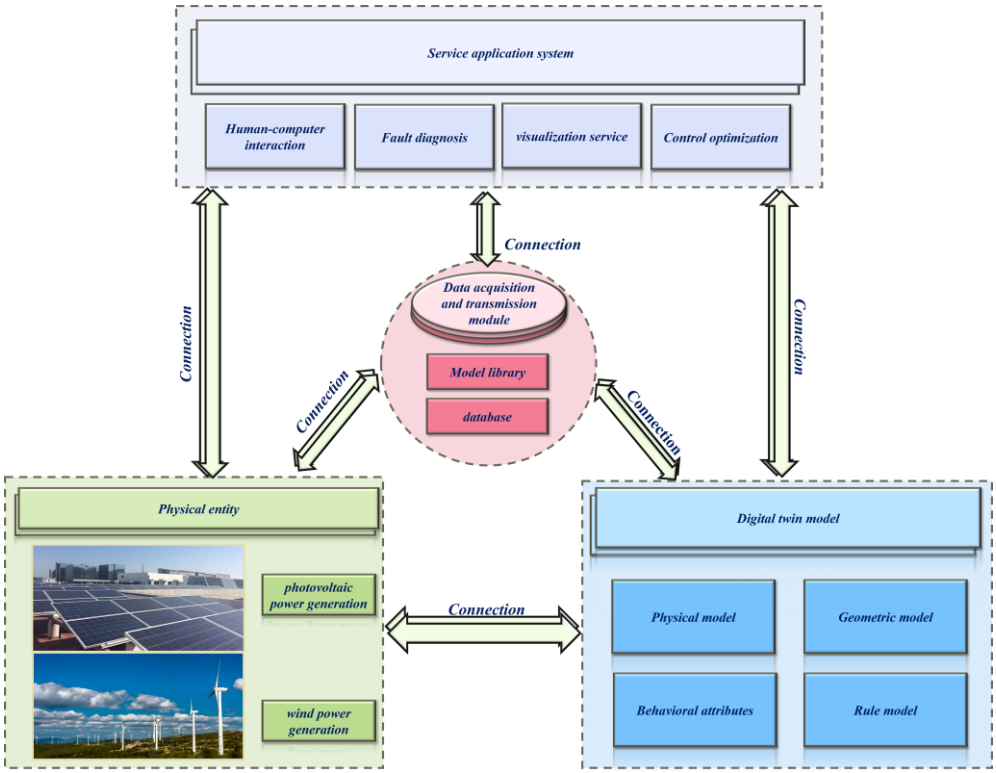

Figure 3. Architecture of the digital twin model for wind-solar integrated power stations.

In summary, within the application scenario of integrated wind-solar storage-charging power stations, the digital twin system has attracted significant attention due to its exceptional data integration and analysis capabilities. This system can collect operational data of power stations in real-time and efficiently, and employ rigorous data cleaning, fusion, and in-depth analysis methods to process massive amounts of data accurately. Building upon this foundation, the present study employs the established digital twin model for wind-solar hybrid power plants to carry out thorough investigations into the node voltage regulation and peak-load shifting control tactics of energy storage power stations. The ultimate objectives are to realize high-efficiency and intelligent operation of the power plants, as well as ensure a stable power supply for the grid.

3. Node voltage control and peak shaving control system based on digital twin

In power systems, with the continuous rise in the proportion of new energy sources, node voltage control and peak shaving/valley filling have become core tasks to ensure the stable operation of the power grid. To this end, this study proposes a node voltage control system integrating digital twin (DT) and PSO. First, the digital twin is used for real-time monitoring and in-depth analysis of plant operation data; in response to the rapid fluctuations of wind and solar output, Copula-VAE is adopted to generate 20 typical scenarios, and the slowly varying uncertainties of load and electricity price are described by Wasserstein fuzzy sets, which together form a two-layer "scenario-set" uncertainty model. Scenarios are injected into the digital twin rolling simulation through sample average approximation (SAA); in the voltage control link, the expected node voltage violation under each scenario is added as an additional penalty term to the objective function, and the original deterministic voltage magnitude constraint is replaced by a scenario-driven worst-case voltage deviation constraint. In the peak shaving/valley filling link, 20 wind-solar scenarios and the extreme load boundaries generated by the Wasserstein set are simultaneously introduced into the power balance constraint. This system can effectively address the voltage fluctuation issues caused by the grid integration of renewable energy sources, improve the overall stability and power quality of the power system, reduce the risk of voltage violation, and ensure the safe and stable operation of the power grid.

3.1. Cluster partitioning algorithm based on PSO

Derived from the observation of foraging patterns in bird flocks, the PSO algorithm emulates the evolution of swarm intelligence observed in nature. It functions as a robust instrument in addressing intricate optimization challenges [16–18]. In the algorithmic framework, each particle signifies a potential problem solution. These particles move through a multidimensional search space at a specific velocity, and their flight paths are influenced by both their individual experiences and the collective information shared within the swarm. Through ongoing adjustments and refinements to their positions, they steadily converge toward the global optimal solution. Key parameters were fixed as follows: swarm size = 50; inertia weight (w) linearly decayed from 0.9 to 0.4 to trade off exploration and exploitation; acceleration coefficients (c_1 and c_2) uniformly set within 1.5–2.0; velocity clamp (Vmax) restricted to 10%–20 % of each variable's range; and maximum iterations = 100. The algorithmic process is illustrated in Figure 4, with its underlying principles and calculation formulas presented as follows:

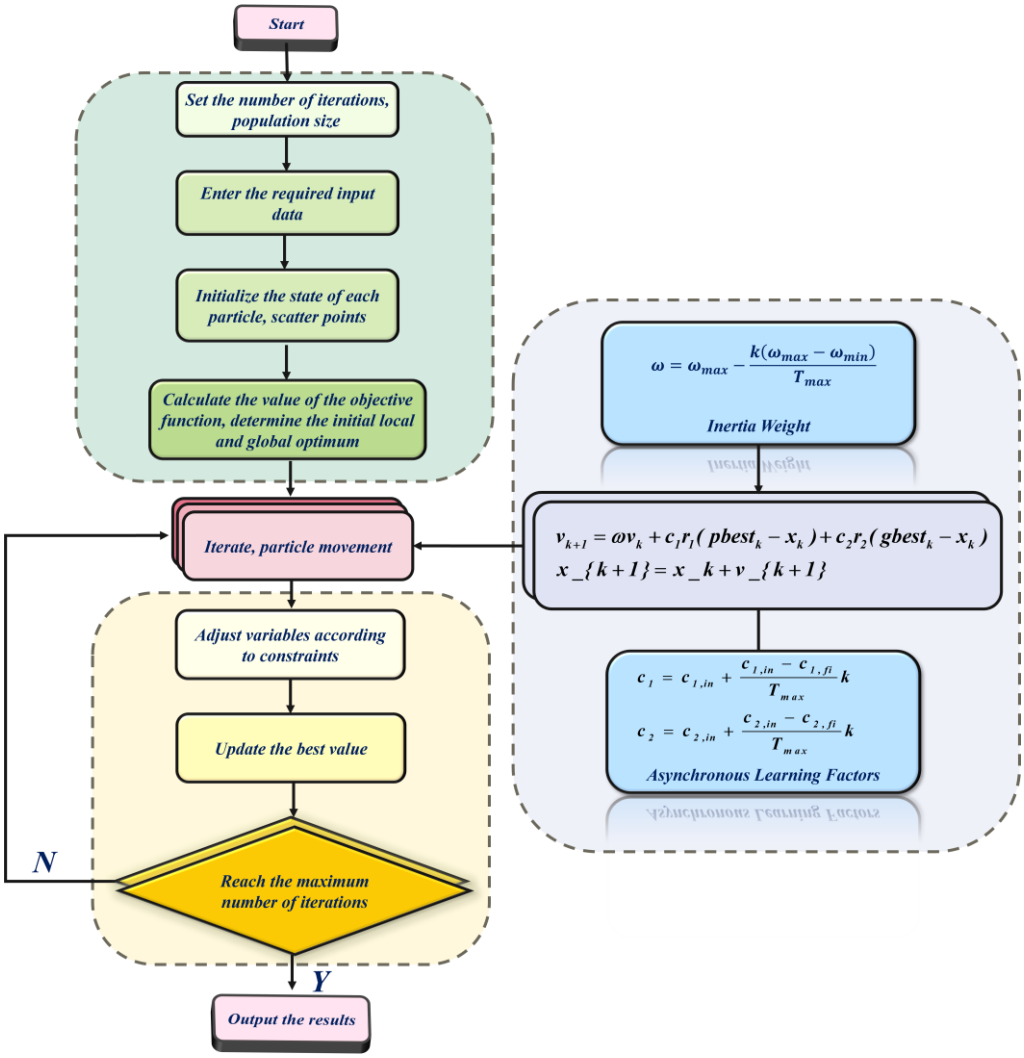

Figure 4. Schematic flow of the PSO algorithm.

(1) Initialization:

In the PSO algorithm, every particle represents a potential solution to the current problem. At the initial stage, every particle within the swarm is allocated a random position and velocity. In this context, the position represents a potential solution, while the velocity governs both the direction and the distance that the particle travels within the search space. The mathematical expressions for the position and velocity are given below:

$$x_i = (x_{i1}, x_{i2}, \cdots, x_{id})^T \tag{1}$$

$$v_i = (v_{i1}, v_{i2}, \cdots, v_{id})^T \tag{2}$$

where $x_{id} \in (x_{\min}, x_{\max})$, represents the minimum limit of the search space, and $x_{\max}$ represents the maximum limit of the search space; $v_{id} \in (v_{\min}, v_{\max})$, where $v_{\min}$ represents the minimum velocity, while $v_{\max}$ stands for the maximum velocity. Positions are drawn uniformly at random across the search space so that every component falls within [x_min, x_max]; initial velocities are likewise sampled uniformly from [v_min, v_max].

(2) Fitness evaluation:

Within the PSO framework, each particle's fitness is assessed through the objective function, which measures its current position. This study selects minimizing node voltage deviation as the objective function, aiming to bring each distribution network node's voltage amplitude as close as possible to the rated value. This not only guarantees power quality but also avoids equipment damage or power outages resulting from voltage overstepping the limits. The objective function can be mathematically formulated as follows:

$$min \sum_{i=1}^{N} |U_i - U_{rated}| \tag{3}$$

where U_i represents the real voltage magnitude of node i, and U_{rated} is the rated voltage. By minimizing the sum of deviations between the voltages of all nodes and the rated voltage, this can effectively enhance the distribution network's voltage stability.

(3) Velocity and position update:

In each iteration process, each particle's personal best and the swarm's global best are documented. Within the PSO algorithm, the formulas governing the velocity and position updates of a particle during the (k + 1)-th iteration are presented below:

$$v_{k+1} = \omega v_k + c_1 r_1 (pbest_k - x_k) + c_2 r_2 (gbest_k - x_k) \tag{4}$$

$$x_{k+1} = x_k + v_{k+1} \tag{5}$$

where x_k denotes the particle's position in the k-th iteration, and x_{k+1} corresponds to the updated position of the particle at the (k + 1)-th iteration; v_k represents the velocity of the particle in the k-th iteration, while v_{k+1} refers to the velocity of the particle in the (k + 1)-th iteration; $pbest_k$ records the optimal solution identified by the particle within the k-th iteration; and $bgest_k$ represents the global optimal solution explored by the entire particle swarm in the k-th iteration.

(4) Inertia weight adjustment:

The inertia weight (w) serves to balance the particles' global and local search abilities. A decreasing inertia weight factor is typically employed, with its formula expressed as follows:

$$w = w_{max} - \frac{k*(w_{max} - w_{min})}{T_{max}} \tag{6}$$

where w denotes the inertia weight, w_{max} and w_{min} represent its upper and lower bounds, respectively, k is the current iteration index, and T_{max} signifies the maximum number of iterations.

(5) Adjustment of learning factors:

The learning factors c_1 and c_2 regulate the extent to which individual experience and group experience affect the velocity of particles, respectively. The adoption of asynchronously changing learning factors enables particles to exhibit a robust self-learning capability during the initial phase of iteration, which promotes global search and a strong learning capacity in the later stage, thereby expediting convergence and optimization. The expressions are as follows:

$$c_1 = c_{1,in} + \frac{c_{1,in} - c_{1,fi}}{T_{max}} k \tag{7}$$

$$c_2 = c_{2,in} + \frac{c_{2,in} - c_{2,fi}}{T_{max}} k \tag{8}$$

where c_1 and c_2 denote the acceleration coefficients, $c_{1,in}$ and $c_{2,in}$ are their respective initial values, and $c_{1,fi}$ and $c_{2,fi}$ represent their final values.

In the node voltage control of distribution networks with new energy integration, the PSO algorithm can regulate the reactive power output of energy storage inverters to achieve optimization. Each particle represents a set of reactive power setting values, and the fitness function evaluates its contribution to node voltage stability. Through iterative optimization, the algorithm finds the optimal reactive power allocation to ensure voltage stability.

3.2. Node voltage control strategy

In power systems incorporating new energy, node voltage stability is vital for ensuring power quality and equipment safety [19]. In this research on node voltage control, minimizing node voltage deviation and minimizing system loss are taken as dual optimization objectives. The specific mathematical expressions are as follows:

$$o_{bj} = min\left(\alpha_1 \sum_{i=1}^{X} |U_{i,t} - U_N| + \alpha_2 \sum_{i=1}^{Y} \sum_{j=1}^{Y} G_{ij} \left(U_{i,t}^2 + U_{j,t}^2 - 2U_{i,t}U_{j,t} \cos\theta_{ij,t} \right) \right) \tag{9}$$

where α_1 and α_2 are the weight coefficients in the objective function (satisfying the normalization constraint $\alpha_1 + \alpha_2 = 1$; α_1 prioritizes the voltage deviation minimization objective, and α_2 focuses on the system loss minimization objective); $U_{i,t}$ denotes the voltage magnitude of the primary node at time t, and U_N refers to the rated voltage, with the unit of p.u.; X and Y represent the count of dominant nodes and the total number of nodes in the distribution network, respectively; $G_{i,j}$ is the line impedance between nodes i and j, with the unit of s; $\theta_{ij,t}$ is the phase angle discrepancy between nodes i and j at time t, with the unit of rad.

Meanwhile, the following constraints should be satisfied when performing the dual optimization of minimizing node voltage deviation and system loss:

(1) Distribution network power flow constraints

$$Q_{i,t} = U_{i,t} \sum_{j=1}^{n} U_{j,t} \left(G_{ij} \sin\theta_{ij,t} - B_{ij} \cos\theta_{ij,t} \right) \tag{10}$$

$$P_{i,t} = U_{i,t} \sum_{j=1}^{n} U_{j,t} \left(G_{ij} \cos\theta_{ij,t} + B_{ij} \sin\theta_{ij,t} \right) \tag{11}$$

where $P_{i,t}$ and $Q_{i,t}$ represent the active and reactive injection powers at node *i* at time t, respectively (KW), and $\theta_{ij,t}$ denotes the voltage phase angle discrepancy between nodes *i* and *j*.

(2) Output constraints of integrated wind-solar distributed generation

$$(P_{i,t}^{PV})^2 + (Q_{i,t}^{PV})^2 = (S_i^{PV})^2 \tag{12}$$

$$\eta_i = \frac{\sum_{t=1}^{T} P_{i,t}^{PV}}{\sum_{t=1}^{T} P_{i,t}^{PVtheory}} \tag{13}$$

$$\eta_i \geq \eta_{min} \tag{14}$$

where S_i^{PV} refers to the capacity of distributed photovoltaic systems at node *i*; η_i represents the photovoltaic utilization rate at node *i* during T; $P_{i,t}^{PVtheory}$ refers to the theoretical output of distributed photovoltaic at node *i* at time *t*; and $\eta_{\min}$ represents the limit value of photovoltaic utilization rate.

(3) Voltage amplitude constraints

$$U^{min} \leq U_{i,t} \leq U^{max} \tag{15}$$

where $U^{\max}$ and $U^{\min}$ represent the respective upper and lower bounds of the node voltage amplitude (KV).

(4) Constraints on branch power

$$P_{ij,t}^{min} \leq P_{ij,t} \leq P_{ij,t}^{max} \tag{16}$$

where $P_{ij,t}^{max}$ and $P_{ij,t}^{min}$ represent the upper and lower bounds of the branch power, respectively (KW).

3.3. Energy storage power plants' peak load regulation control strategy

In the field of peak shaving control in power systems, the digital twin system plays a crucial role. Boasting the capabilities of precisely forecasting power grid loads and real-time monitoring of new energy generation, this approach uses the PSO algorithm to optimize energy storage capacity configuration. Consequently, it allows for the pre-establishment of rational charge-discharge strategies for energy storage systems [20]. During periods of peak grid load, the energy storage system releases electrical energy promptly following these predetermined strategies. This not only eases grid operational pressure but also significantly boosts its operational stability and reliability. Figure 5 depicts the battery energy storage system (BESS)'s electrical principle. A detailed analysis of this schematic further confirms the energy storage system's role in peak shaving control. In doing so, it lays a robust theoretical foundation for optimizing the peak shaving control strategies of energy storage power stations.

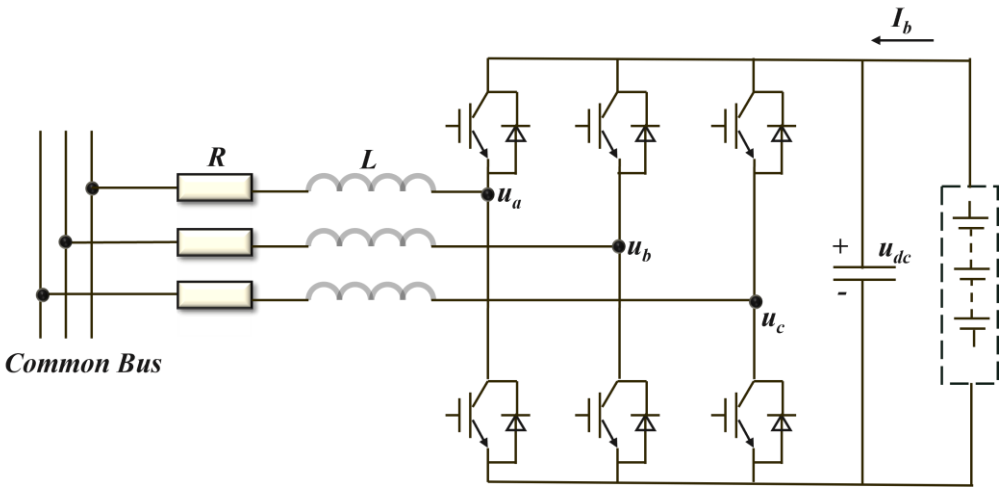

Figure 5. Schematic diagram of BESS.

The load rate indicates the proportion of a transformer's actual load to its capacity. When the system load rate approaches the average value with small fluctuations, the indicators of overload and voltage over-limit decrease, and the safety level improves. From the perspective of safety, the load rates of the main transformers in each energy storage power station should be similar, which not only ensures safety but also improves equipment utilization. The balance level is evaluated using the transformer load rate's standard deviation; a smaller standard deviation signifies a more balanced load. The expression for the balance degree χ of the transformer load rate is as follows:

$$min\,\chi = \sum_{t}\sum_{i}\sqrt{\frac{1}{n}\left(\mu_{it} - \mu_{ave,t}\right)^2} \tag{17}$$

where n denotes the total count of energy storage power stations, and for the *i-th* one among them, μ_{it} is the load rate of the connected substation during period t; $\mu_{ave,t}$ is the average load rate of multiple energy storage power stations during period t.

The grid-connected peak shaving control strategy is designed to realize peak clipping and valley filling while guaranteeing load stability, thereby reducing the stress on the power grid during peak load periods. The setting of charging targets needs to be based on the load level and BESS capacity and comply with relevant constraints.

(1) Load level and BESS capacity constraints

$$E_{rem} + \sum_{i=1}^{N_1} P_{ch,i} \times \Delta t \le E_1 \tag{18}$$

$$0 \le P_{ch,i} \le P_{ch,max} \tag{19}$$

where $P_{ch,i}$ represents the charging power at moment t; Δt represents the period for switching charging power; E_{rem} is the residual capacity of the energy storage battery before charging; E_1 refers to the secure charging capacity of the BESS; $P_{ch,max}$ is the maximum charging power allowed for BESS; and N_1 is

the number of charging intervals.

(2) Constraints on stable output of generator sets

For a generator set in operation, its actual generating output must fall within the range that is higher than its minimum stable operating output and lower than its maximum generating capacity.

$$P_{g,k}^{min} \le P_{g,k} \le P_{g,k}^{max}, \quad k \in G_I \tag{20}$$

where $P_{g,k}^{min}$ and $P_{g,k}^{max}$ represent the minimum and maximum output thresholds of the generator *k*, respectively, and G_I denotes the set of all generators in the system.

(3) State of charge constraints of energy storage power stations

$$SOC_{BESS_n}^{min} \le SOC_{BESS_n} \le SOC_{BESS_n}^{max} \tag{21}$$

where, for the nth energy storage power station, there are clear boundary constraints on its state of charge, with $SOC_{BESS_n}^{min}$ as the minimum limit and $SOC_{BESS_n}^{max}$ as the maximum limit.

(4) Energy balance constraints of energy storage power stations

$$E_{BESS_n}^{cha} - E_{BESS_n}^{dis} < \varepsilon \tag{22}$$

where $E_{BESS_n}^{cha}$ represents the total charging energy of the *n-th* energy storage power plant, and $E_{BESS_n}^{dis}$ stands for the total discharged energy of the n-th energy storage power plant; ε is a constant close to zero.

3.4. Simulation example based on the IEEE 33-bus system

Addressing the core requirements (real-time performance, adaptability to complex constraints, and engineering practicality) of node voltage control and peak shaving optimization for wind-solar storage-charging-integrated power stations, this paper takes the minimization of power grid peak-valley difference as the core evaluation index and systematically compares the performance adaptability of four mainstream advanced algorithms: genetic algorithm (GA), whale optimization algorithm (WOA), deep reinforcement learning (DRL), and PSO. Specific comparisons are shown in Table 1.

Table 1. Comparison of various optimization algorithms.

Algorithm type	Advantages	Core limitations (in the context of power grid peak-valley difference optimization)	Engineering adaptability
GA	Strong robustness in global optimization and ability to cover the solution space of multiple constraints.	High computational cost and relatively slow convergence speed, leading to lagged real-time optimization response for peak-valley difference and difficulty in matching the dynamic peak shaving requirements of power stations.	Although GA has excellent global optimization capability, its shortcoming of slow convergence speed prevents it from meeting the real-time optimization requirements of peak-valley difference, making it difficult to adapt to the dynamic peak shaving scenarios of power stations [21,22].
WOA	High optimization efficiency in low-dimensional single-objective optimization scenarios.	Prone to oscillation and insufficient stability in high-dimensional multi-node and multi-constraint scenarios, resulting in large fluctuations in peak-valley difference optimization accuracy and failure to ensure consistent peak shaving effects.	Due to insufficient stability in the wind-solar storage-charging system with high dimensions and multiple constraints, WOA directly affects the reliability of peak shaving effects and has limited engineering practicality [23,24].
DRL	Potential for adaptive learning in dynamic environments.	Relies on massive sample training with limited generalization ability; insufficient reliability of real-time decision-making for peak-valley difference optimization under dynamically changing new energy operating conditions and high engineering implementation cost.	The generalization ability defects and sample dependence of DRL make it difficult to achieve real-time decision-making for peak-valley difference optimization and low-cost engineering implementation under scenarios with dynamically changing new energy operating conditions [24–26].
PSO	Simple principle, high computational efficiency, and easy real-time data interaction with digital twin systems.	No obvious shortcomings; can balance the real-time performance and accuracy of peak-valley difference optimization under multi-objective constraints, and is adaptable to dynamic peak shaving scenarios.	The PSO algorithm not only has high computational efficiency to quickly respond to the dynamic optimization needs of peak-valley difference but can also stably approach the global optimal solution under multi-constraint conditions through the information collaboration mechanism between individuals and the swarm [27–29].

Based on the systematic review and qualitative analysis of relevant literature, and after careful consideration of multiple aspects, the PSO algorithm is ultimately selected as the core optimization tool. Its advantages are highly consistent with the requirements of this study. First, in terms of

algorithm principles, PSO simulates the search mechanism of swarm intelligence, possessing both global exploration and local convergence capabilities. Compared with the crossover and mutation mechanisms of GA, it is more concise and efficient; unlike DRL, it does not rely on massive sample training and can quickly respond to dynamic scheduling needs. Second, regarding scenario adaptability, PSO performs prominently in multi-constraint optimization scenarios of renewable energy power stations, effectively balancing the dual objectives of voltage control and peak-valley difference optimization, while avoiding the oscillation defect of WOA in high-dimensional scenarios and the insufficient generalization ability of DRL. Third, from the perspective of engineering practicality, PSO has flexible parameter adjustment and can seamlessly interface with the real-time data interaction of the digital twin system. This feature is highly compatible with the core framework of "virtual-physical mapping-rolling optimization" in this study, which is an irreplaceable advantage of other algorithms. Furthermore, this paper further compares the proposed strategy with the hybrid game-theoretic stochastic robust optimization methods for multi-energy microgrids, which have attracted much attention in the field of current dynamic scheduling. Such hybrid game-theoretic methods excel in coupling detailed uncertainty modeling and two-layer coordination and have achieved certain results in addressing the complexity of multi-energy interaction [30]. However, due to the complex construction of their game-theoretic framework and cumbersome solution process, they often suffer from high computational complexity. The time-consuming iterative process is difficult to meet the minute-level rolling update requirements for the scheduling of integrated wind-solar storage-charging power stations. Meanwhile, PSO performs prominently in multi-constraint optimization scenarios of renewable energy power stations, effectively balancing the dual objectives of "minimum voltage deviation + minimum system loss" while avoiding the oscillation defect of WOA in high-dimensional scenarios and the insufficient generalization ability of DRL. Contemporary mainstream integrated energy scheduling frameworks (such as multi-timescale coordinated scheduling and hierarchical scheduling of integrated energy stations) mostly adopt the offline preset hierarchical logic of "day-ahead planning–intraday adjustment–real-time correction". There is a delay in interlayer coordination, making it difficult to adapt to the random fluctuations of renewable energy output [31,32]. Therefore, this paper ultimately selects the PSO algorithm as the core optimization tool for reactive power allocation and optimization of energy storage charging and discharging plans in integrated wind-solar storage-charging power stations.

To verify the proposed node voltage regulation and power station peak shaving control system (integrating digital twin and PSO), a simulation analysis on a modified IEEE 33-node distribution network is conducted. The system's single-line diagram is illustrated in Figure 2, while the clustering results are summarized in Table 2. This distribution network features 33 nodes and 32 branches arranged in a radial structure. The total line length is 11.957 km, the rated voltage is 12.66 kV, and the base power is 100 MVA. All branch parameters and node load data adhere to IEEE specifications. To simulate scenarios with new energy integration, distributed generation and energy storage systems are connected to specific nodes: photovoltaic (PV) systems reside at nodes 5, 17, 22, 26, 28, and 32; wind turbines connect to nodes 10, 15, and 20; and distributed energy storage systems (ESS) are at nodes 13, 20, and 32. Each ESS has a rated power of 0.15 MW, a 2 MWh capacity, a state of charge (SOC) operating range of 0.1–0.9, and an initial SOC of 0.5. The distribution network operates at a 12.66 kV rated voltage, allowing node voltage to deviate by ± 5% from this nominal value.

Table 2. Partition results of the IEEE 33-node system.

Partition number	Node number
D_1	1–25
D_2	26–28
D_3	29–33

In a thorough examination of the voltage regulation performance of the proposed strategy, given that photovoltaic systems, wind power generation systems, and load fluctuations within the distribution network all exert an impact on voltage magnitudes, 24-h datasets of photovoltaic output, wind power output, and load in a specific region were chosen for the research. The corresponding variation curves are illustrated in Figure 6. It is observed that the photovoltaic power output has significant time-varying characteristics, while the wind power output is relatively stable, basically within a certain range with small fluctuations. The node voltage is impacted more profoundly by photovoltaic power generation, showing an obvious dynamic change trend over time.

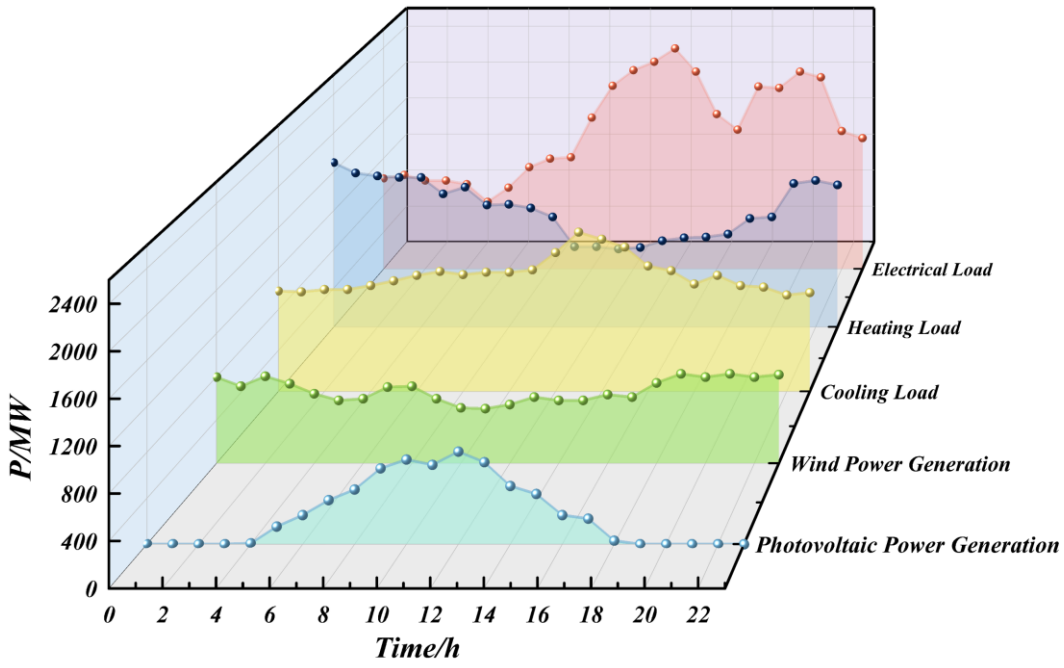

Figure 6. Load and new energy output in a certain area.

In simulations, the data collection interval and simulation step size are both 1 min, with voltage restricted between 0.95 and 1.05 p.u. and clear upper/lower bounds. Experimental results are presented in Figure 7. Figure 7a depicts the 24-h voltage profile of a selected node; Figure 7b shows the nodal voltage distribution at a specific instant. When the traditional control strategy is adopted, the node voltage exceeds the upper limit at 9 o'clock, and reaches a peak of 1.1 p.u. at 11 o'clock, with poor voltage stability. However, upon implementation of the control strategy put forward in this study, the node voltage, despite exhibiting an upward tendency, remains strictly within the defined limits, thus successfully preventing voltage over-limit issues. At 19 o'clock, due to load factors, the node voltage falls below the lower threshold, and then as the load gradually decreases, the voltage returns to normal

until 23 o'clock. In contrast, under the action of the control methodology employed in this research, although the node voltage has a downward trend, there is no over-limit phenomenon, showing good voltage regulation ability.

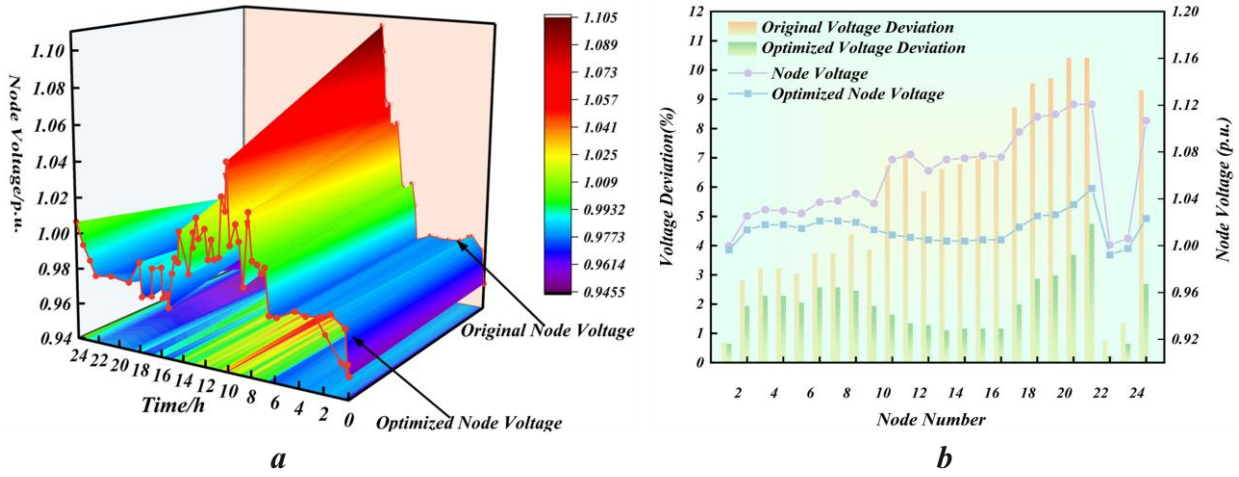

Figure 7. Node voltage curve: (a) 24-h voltage profile of a given node; (b) voltage snapshot of specific nodes at a given instant.

Further comparing the two control strategies, the node voltage fluctuation range under the conventional control approach is ± 5%, and the number of voltage over-limits is as high as 8 times. In contrast, the approach proposed in this study remarkably narrows the range of node voltage fluctuations to within ± 2% and reduces the number of voltage over-limits to 1 time. Results show that the proposed strategy always maintains node voltage within the set range. It effectively boosts distribution network voltage stability and shows significant advantages in addressing voltage fluctuation issues.

As shown in Figures 8a and 8b, based on the one-year operation data of wind farms and photovoltaic power stations in Changchun City and the surrounding areas of Jilin Province, China, five representative scenarios (Scenario 1–5) were identified. The data preprocessing steps are as follows: (1) Linear interpolation was used to fill missing values (accounting for < 0.3% of the total data), (2) abnormal data was removed using the 3σ criterion, (3) data was normalized to the [0,1] interval to adapt to algorithm input requirements, and (4) K-means clustering analysis was performed on the annual data, and five cluster centers covering typical days in winter, summer, spring, and autumn, as well as extreme sunny days and extreme rainy days, were selected as representative scenarios. Each scenario represents a type of situation with similar output characteristics, covering the changes in new energy output under different seasons and weather conditions. Drawing upon these representative scenarios, an in-depth investigation into peak load shaving is carried out for the energy storage power stations located in this area. To validate the efficacy of the proposed approach, within the chosen scenarios, the traditional energy storage peak shaving method and the peak shaving method combining digital twin and PSO strategy employed in the article are compared, and the results are shown in Figure 8c.

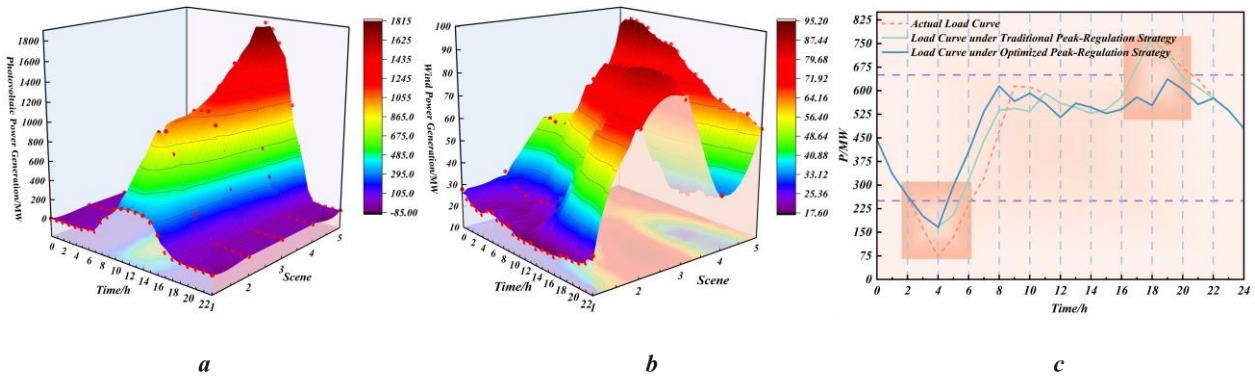

Figure 8. Renewable generation and peak-shaving performance for the studied region: (a) PV output curves under different scenarios; (b) wind-power output curves under different scenarios; (c) comparison of peak-shaving effects among different strategies.

From the experimental results, although the traditional energy storage peak shaving method can alleviate the load peak-valley difference to a certain extent, it is limited by its limitations, and the peak shaving effect is poor when facing complex and changeable new energy output scenarios. The proposed digital twin and PSO strategy can efficiently utilize energy storage resources, achieving better peak shaving and valley filling via accurate modeling and intelligent optimization. Under the conventional peak-shaving strategy, the 24-h system-wide equivalent load exhibits a mean peak-to-valley difference of 30%. After applying the proposed digital twin-PSO-based approach, this figure drops to 15%—a 50% reduction. Concurrently, the standard deviation, mean absolute error, and root-mean-square error decrease from 4.8%, 4.5%, and 5.2% to 2.3%, 2.0%, and 2.4%, respectively. To verify the statistical significance of the results, this study adopts an independent two-sample t-test (two-tailed test). The algorithm was run independently 30 times to eliminate random errors. The null hypothesis H_0 is as follows: 'there is no significant difference in the optimization effect between the proposed strategy and the traditional strategy'. The alternative hypothesis H_1 is as follows: 'the optimization effect of the proposed strategy is significantly better than that of the traditional strategy'. The degrees of freedom (df = 68.3) were calculated using the Welch-Satterthwaite formula, with a test statistic of t = 8.62 and a final p-value < 0.01. The null hypothesis is rejected at the 99% confidence level, proving that the statistical significance of the optimization effect can be independently verified. This improvement optimizes energy storage power stations' peak shaving efficiency and significantly enhances the entire power system's operational stability and cost-effectiveness. It strongly supports new energy consumption and grid safe/stable operation, demonstrating the proposed method's practical value and advantages.

In summary, the proposed dynamic scheduling strategy for wind-solar storage-charging-integrated power stations based on digital twin technology shows significant advantages in improving new energy power station operational efficiency, grid stability, and system reliability. By building a digital twin model, it realizes all-around real-time monitoring, in-depth simulation, and intelligent optimal control of the power station. Regarding node voltage regulation and peak load management, the PSO algorithm effectively reduces node voltage fluctuations and optimizes energy storage systems' charge-discharge schedules. Simulation results show that the proposed strategy reduces node voltage fluctuation from ± 5% to ± 2%, cuts over-limit instances from 8 to 1, and lowers the grid's peak-valley difference

from 30% (traditional strategy) to 15%. Looking ahead, as digital twin technology continues to advance, its application prospects in power systems will become broader, offering robust technical backing for the construction of a clean, efficient, and reliable energy system [33].

4. Conclusions

The dynamic scheduling approach for integrated wind-solar storage-charging power stations presented in this study, which leverages digital twin technology, shows considerable benefits in enhancing the operational efficiency of new energy power stations, stabilizing the power grid, and boosting system dependability.

(1) The digital twin model built in this paper integrates real-time wind power, photovoltaic, and energy storage system data for accurate physical entity and virtual model mapping and real-time interaction. This model features functions of real-time monitoring, in-depth simulation analysis, and intelligent optimal control, enabling it to dynamically reflect the operating status of physical entities. It provides an innovative approach for new energy power station optimization management, promoting the new energy sector's development and enhancing wind-solar-integrated power station operational levels.

(2) In node voltage control, the digital twin system combines with the PSO algorithm, targeting minimal node voltage deviation as the objective function. It perpetually tracks grid voltage levels in real-time, accurately captures grid voltage dynamic changes, and dynamically adjusts the energy storage system's reactive power output based on its charge-discharge characteristics. Simulation results indicate that, in comparison with the original voltage, the proposed strategy can notably narrow the node voltage fluctuation range from ± 5% to ± 2% and reduce the number of voltage over-limits from 8 to 1. This fully proves that the strategy maintains node voltage within the set range, effectively enhances distribution network voltage stability, reduces voltage over-limit risks, and ensures the power system's safe and stable operation. In future work, I will couple the Transformer-based short-term voltage-stability risk framework with a multivariate spatiotemporal model of wind, solar, load, and PMU data to generate a voltage-instability-probability-versus-time trajectory. When embedded as a soft constraint in receding-horizon optimization, this trajectory is projected to cut daily voltage-limit violations from one to ~0.2 and curb storage ageing induced by frequent power adjustments.

(3) Regarding the peak shaving control strategy, by using the digital twin system's simulation analysis capabilities and the PSO algorithm, a comprehensive analysis of the grid load curve and new energy unit output characteristics is conducted. The proposed digital twin/PSO two-stage rolling framework embeds for the first time a renewable-generation scenario library into real-time simulation, allowing minute-level refresh of the storage day-ahead schedule and cutting the peak-valley gap from 30% to 15%; the framework remains robust for grids with > 50% renewable penetration, offering a replicable simulate–optimize–resimulate closed-loop paradigm.

Use of AI tools declaration

The author team used ChatGPT (Version GPT-4, developed by OpenAI) for: (1) Assisting in drafting the initial Introduction; (2) Polishing the language of the "Related Work" and Discussion sections. Any AI-generated content was subsequently rewritten, fact-checked against the literature, and corrected by the authors to ensure scientific accuracy. No AI tools were used in other parts of the research. All authors bear full responsibility for the scientific validity, originality, and compliance of

the entire manuscript.

Conflict of interest

The authors declare no conflicts of interest.

Acknowledgements

This work was supported by a project grant from "Research on Advanced Technology Application in Charging and Swapping Infrastructure in Jilin Province" of Power Grid Enterprises in the New Era of Jilin Province Changchun Electric Power Survey and Design Institute Co., Ltd (Grant No. SGJLKC00ZHJS2500222).

Author contributions

Xiancheng Cui: Conceptualization, Methodology, Investigation, Validation, Writing—Original Draft Preparation, Writing—Review & Editing; Xiaoming Lu: Investigation, Modeling, Methodology, Validation, Writing—Methodology, Interpretation of Results; Yiwen Yao: Investigation, Methodology, Data Curation, Writing—Results; Xin Xu: Investigation, Data Curation, Methodology, Visualization, Writing—Discussion; Meihan Liu: Literature Curation, Conceptualization, Writing—Review & Editing; Jingjie Zhao (corresponding author): Supervision, Conceptualization, Writing—Review & Editing, Project Administration. All authors have read and approved the final version of the manuscript and agree to be accountable for all aspects of the work.

References

1. Zhu Y, Lan M (2023) Digital economy and carbon rebound effect: evidence from Chinese cities. *Energy Econ* 126: 106957. https://doi.org/10.1016/j.eneco.2023.106957
2. Jiang D, Zhang S, Pang K (2025) Data center temperature control method based on multi-parameter model-free adaptive control strategy. *Energies* 13: 2360. https://doi.org/10.3390/pr13082360
3. Arora R (2020) Energy, exergy and exergoeconomic analyses and optimisation of 137 MW gas power station implementing MOPSOCD. *Int J Energy Technol Policy* 16: 327−352. https://doi.org/10.1504/IJETP.2020.107954
4. Ismail F B, Al-Faiz H, Hasini H, et al. (2024) A comprehensive review of the dynamic applications of the digital twin technology across diverse energy sectors. *Energy Strategy Rev* 52: 101334. https://doi.org/10.1016/j.esr.2024.101334
5. Liu Z, Li M, Ji W (2025) Development and application of a digital twin model for net zero energy building operation and maintenance utilizing BIM-IoT integration. *Energy Build* 328: 115170. https://doi.org/10.1016/j.enbuild.2024.115170
6. Zhao X, Zhang Y (2024) Integrated management of urban resources toward net-zero smart cities considering renewable energies uncertainty and modeling in digital twin. *Sustainable Energy Technol Assess* 64: 103656. https://doi.org/10.1016/j.seta.2024.103656

7. Singh A, Aujla GS, Jindal A, et al. (2025) Leveraging digital twins for anomaly detection and adaptive healing in software-defined IoT. *2025 IEEE International Conference on Communications Workshops (ICC Workshops)*, Montreal, QC, Canada, 899−904. https://doi.org/10.1109/ICCWorkshops67674.2025.11162268
8. Parada Contzen M (2024) A distributed double-layer control algorithm for medium voltage regulation and state of charge consensus of autonomous battery energy storage systems in distribution networks. *J Energy Storage* 103: 114314. https://doi.org/10.1016/j.est.2024.114314
9. Inaolaji A, Wu X, Roychowdhury R, et al. (2024) Optimal allocation of battery energy storage systems for peak shaving and reliability enhancement in distribution systems. *J Energy Storage* 95: 112305. https://doi.org/10.1016/j.est.2024.112305
10. Liang Y, Zhang J, Shi Z, et al. (2024) A fault identification method of hybrid HVDC system based on wavelet packet energy spectrum and CNN. *Electronics* 13: 2788. https://doi.org/10.3390/electronics13142788
11. Ouyang T, Zhang M, Qin P, et al. (2025) Flow battery energy storage system for microgrid peak shaving based on predictive control algorithm. *Appl Energy* 356: 122448. https://doi.org/10.1016/j.apenergy.2023.122448
12. Yan R, Xu Y (2025) Multi-objective and multi-agent deep reinforcement learning for real-time decentralized volt/VAR control of distribution networks considering PV inverter lifetime. *IEEE Trans Power Syst* 40: 1558−1569. https://doi.org/10.1109/TPWRS.2024.3452154
13. Yin X, He Q, Peng S, et al. (2025) A health state prediction model for aeroengine based on multi-attribute belief rule base with considering monitoring error. *Inter J Fuzzy Syst* 27: 1072−1095. https://doi.org/10.1007/s40815-024-01808-x
14. Ye X, Zhou Z, Cheng Y (2025) A detection method for electricity theft behaviour in low-voltage power stations: Multi-source data fusion. *Int J Energy Technol Policy* 20: 36−50. https://doi.org/10.1504/IJETP.2025.144303
15. Zhang B, Cao D, Hu W, et al. (2024) Physics-informed multi-agent deep reinforcement learning enabled distributed voltage control for active distribution network using PV inverters. *Int J Electr Power Energy Syst* 155: 109641. https://doi.org/10.1016/j.ijepes.2023.109641
16. Pradhan A, Das A, Bisoy SK (2025) Modified parallel PSO algorithm in cloud computing for performance improvement. *Cluster Comput* 28: 131. https://doi.org/10.1007/s10586-024-04722-x
17. Yatim HM, Mohd-Ghazali N, Mohamad M, et al. (2023) Two-phase heat transfer microchannel system identification with Particle Swarm Optimization (PSO) approach. *Int J Air-Cond Ref* 31: 13. https://doi.org/10.1007/s44189-023-00029-5
18. Nobile MS, Cazzaniga P, Besozzi D, et al. (2018) Fuzzy self-tuning PSO: A settings-free algorithm for global optimization. *Swarm Evol Comput* 39: 70−85. https://doi.org/10.1016/j.swevo.2017.09.001
19. Gu J, Huang W, Yan C, et al. (2025) Low-carbon economic dispatch of integrated energy systems with electric vehicle participation. *Electronics* 14: 4557. https://doi.org/10.3390/electronics14234557
20. Amiri MM, Aghajan-Eshkevari S, Rahimi MA, et al. (2024) A review on utilization of electric vehicles for mitigating the power quality issues in power systems. *Power Quality-New Insights*, IntechOpen. https://doi.org/10.5772/intechopen.1003592

21. Hameed S, Tanoli IK, Khan TA, et al. (2025) A novel self-healing genetic algorithm for optimizing single objective flow shop scheduling problem. *Arab J Sci Eng* 50: 7069–7084. https://doi.org/10.1007/ s13369-024-09240-x
22. Magalhães R, Sousa JMC, Vieira SM (2025) A heuristic guided genetic algorithm applied to dual resource job shop scheduling. *Mathematics* 13: 3116. https://doi.org/10.3390/math13193116
23. Mezaghrani A, Debakla M, Djemal K (2025) Parallel whale optimization algorithm-kmeans for image segmentation using multiprocessing. *2025 International Symposium on iNnovative Informatics of Biskra (ISNIB)*, Biskra, Algeria, 1–6. https://doi.org/10.1109/ISNIB64820.2025.10983906
24. Nadimi-Shahraki MH, Farhanginasab H, Taghian S, et al. (2024) Multi-trial vector-based whale optimization algorithm. *J Bionic Eng* 21: 1465–1495. https://doi.org/10.1007/s42235-024-00493-8
25. Sonie O (2022) Conversational recommender system using deep reinforcement learning. *Proceedings of the 16th ACM Conference on Recommender Systems. Presented at the RecSys '22: Sixteenth ACM Conference on Recommender Systems*, ACM, Seattle WA USA, 718–719. https://doi.org/10.1145/3523227.3547376
26. An J, Si GY, Zhang L, et al. (2022) Stereoscopic projection policy optimization method based on deep reinforcement learning. *Electronics* 11: 3951. https://doi.org/10.3390/electronics11233951
27. Babiarz A (2023) PID controller tuning for Capsubot with standard and fractional-order PSO algorithm. *2023 27th International Conference on Methods and Models in Automation and Robotics (MMAR)*, Międzyzdroje, Poland, 297–302. https://doi.org/10.1109/MMAR58394.2023.10242513
28. Jain M, Saihjpal V, Singh N, et al. (2022) An overview of variants and advancements of PSO algorithm. *Appl Sci* 12: 8392. https://doi.org/10.3390/app12178392
29. Jin B, Liu Y, Cai J (2024) An overview of PSO method for PA optimization. *2024 IEEE Asia-Pacific Microwave Conference (APMC)*, Bali, Indonesia, 516–518. https://doi.org/10.1109/APMC60911.2024.10867532
30. Gao Y, Tahir M, Siano P, et al. (2025) A bi-level hybrid game framework for Stochastic Robust optimization in multi-integrated energy microgrids. *Sustainable Energy Grids Networks* 44: 102024. https://doi.org/10.1016/j.segan.2025.102024
31. Liu J, Wang Z, Zang X, et al. (2024) Data-driven dynamic assessment method of wind farm frequency characteristics based on state space mapping. *CSEE Power Energy Syst* 11: 1018–1029. https://doi.org/10.17775/CSEEJPES.2023.02430
32. Li B, Zheng D, Li B, et al. (2024) Research on low voltage ride-through strategies for doubly-fed wind farms during asymmetric faults. *Int J Electr Power Energy Syst* 160: 110138. https://doi.org/10.1016/j.ijepes.2024.110138
33. Li Y, Cao J, Xu Y (2024) Deep learning based on Transformer architecture for power system short-term voltage stability assessment with class imbalance. *Renewable Sustainable Energy Rev* 189: 113913. https://doi.org/10.1016/j.rser.2023.113913